Journal of Physics: Conference Series

PAPER • OPEN ACCESS

CFD simulation and geometric optimization of a novel baffle heat sink for power electronics cooling

To cite this article: I T'Jollyn *et al* 2024 *J. Phys.: Conf. Ser.* **2766** 012175

Journal of Physics: Conference Series **2766** (2024) 012175 doi:10.1088/1742-6596/2766/1/012175

CFD simulation and geometric optimization of a novel baffle heat sink for power electronics cooling

I T'Jollyn[1,2,3], J Rogiers[2,3], J Nonneman[2,3] and M De Paepe[2,3]

[1] Energy and Materials in Infrastructure and Buildings (EMIB) research group, University of Antwerp, Groenenborgerlaan 171, Antwerp, Belgium
[2] Sustainable Thermo-Fluid Energy Systems research group, Ghent University, Sint-Pietersnieuwstraat 41, Ghent, Belgium
[3] FlandersMake@UGent – Core lab MIRO, Gaston Geenslaan 8, Leuven, Belgium

E-mail: Ilya.TJollyn@UAntwerpen.be

Abstract. The electric drivetrain of an electric vehicle typically has two fluid circuits: an oil circuit for lubrication and a water-glycol circuit for cooling. Eliminating the water-glycol circuit can result in a more compact and lighter drivetrain. However, this requires the drivetrain components to be cooled with oil as coolant, which has inferior heat transfer properties compared to water-glycol mixtures. This is particularly challenging for the power modules in the power electronics unit, which exhibit some of the highest heat fluxes in the drivetrain. This study focusses on the design and optimization of a novel type of heat sink for laminar flows with baffles to guide the flow in four different directions. This has two main advantages: the baffles act as fins and increase the heat transfer area and they introduce a swirling motion in the oil thereby disturbing the boundary layers continuously. Computational fluid dynamics simulations using Ansys Fluent are performed to evaluate the thermohydraulic performance of the heat sink. The influence of design parameters such as the height and thickness of both fins and baffles and the baffle spacing in horizontal, upward and downward direction was evaluated by simulations with several combinations of the design space, considering manufacturing constraints. The optimization of the design showed that the fin thickness, horizontal baffle spacing and baffle length should be as small as possible, while there were optimal values for fin height, upward and downward baffle spacing, streamwise baffle spacing and baffle thickness. The simulations show that the thermal resistance of the baffle heat sink can be 19% lower than that of a benchmark pin fin heat sink at equal pumping power.

1. Introduction

Electric vehicles (EVs) are rapidly gaining traction in the automotive market due to their reduced environmental footprint, chiefly stemming from lower emissions [1]. Despite this, a significant drawback of current-generation EVs is their limited driving range [2]. One potential remedy is to enhance the compactness of the drivetrain, as a more compact and lighter drivetrain contributes to superior overall system efficiency. However, this adjustment results in increased power dissipation per unit volume, posing challenges in cooling the drivetrain components. This drivetrain typically encompasses the battery, motor, gearbox, and power electronics [3]. The power electronics transform the DC voltage and current from the batteries to an AC waveform to power the electric motor.

Journal of Physics: Conference Series **2766** (2024) 012175	doi:10.1088/1742-6596/2766/1/012175

Conventionally, forced liquid cooling utilizing a water-glycol mixture is employed to cool the power electronics [4]. Consequently, two distinct liquid circuits are integrated into the drivetrain: an oil lubrication circuit and a water-glycol coolant circuit. An approach to enhance drivetrain compactness involves merging these circuits by utilizing lubrication oil to cool both the power electronics and motor. Nonetheless, the thermal properties of oil (lower thermal conductivity and specific heat capacity and higher viscosity) are inherently inferior to those of water-glycol in terms of heat transfer efficiency.

For the cooling of the power modules in the power electronics unit, this poses significant challenges as very high heat fluxes occur here. Conventional designs (for water-glycol) are not optimal for oil flows, as the flows will typically be laminar compared to turbulent for water-glycol. The 3D flow behaviour which is inherent to turbulent flows thus needs to be introduced by the heat sink geometry for laminar flow, to avoid the building up of thermal boundary layers which inhibit effective heat transfer. In this work, a novel geometry consisting of baffles in four directions is introduced. Using computational fluid dynamics (CFD), the performance of the baffle heat sink is analysed and the geometry is optimized.

2. Simulation setup

2.1. Geometry

The novel baffle heat sink consists of multiple parallel channels with baffles in four directions. The baffles guide the flow to the right, bottom, left and top repeatedly introducing a swirling motion to avoid the buildup of thick thermal boundary layers. Furthermore, the baffles add heat transfer area and thus act as fins.

Figure 1 shows a unitary cell of the heat sink. The entire heat sink consists of multiple of these cells in parallel and series. In the simulations, only the unitary cell is used to reduce computational time. The results are afterwards scaled to the full size of the heat sink, which has a width of 56 mm and a streamwise length of 57 mm, based on the size of a commercial power module.

The baffles pointed towards the left, right and top can be manufactured by milling, the baffle pointing towards the bottom should in this case be inserted by a separate part at the top. Another option is to use additive manufacturing, in which case the entire geometry can be made out of one piece. In this work, the heat sink is assumed to comprise of two parts. As there will be a considerable thermal contact resistance between both parts, heat transfer through the top part is considered negligible and thus not taken into account in the simulations.

Several dimensions of this geometry can be altered (figure 2): the fin thickness (A), horizontal baffle spacing (B), baffle length (C), streamwise baffle spacing (D), baffle thickness (E), vertical baffle spacing downward (F), vertical baffle spacing upward (G) and baffle height (H). The radius of the fillets (I) is always equal to half the streamwise baffle spacing (D).

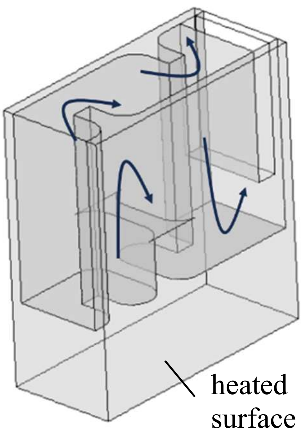

Figure 1. Unitary cell of baffle heat sink indicating flow directions.

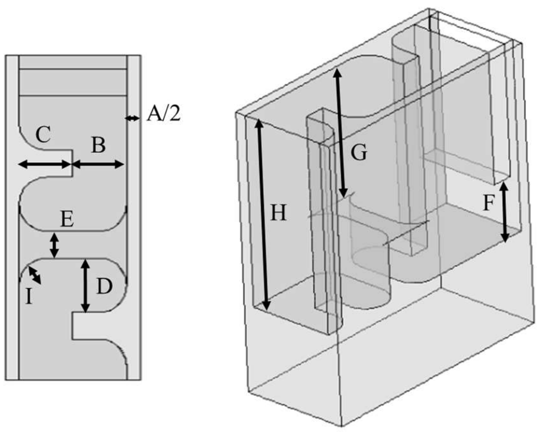

Figure 2. Geometric parameters of baffle heat sink.

2.2. Boundary conditions
As the unitary cell is repeated several times in the streamwise direction, a periodic boundary condition is used for inlet and outlet, where the outlet velocities and scaled temperatures are wrapped to the inlet. The temperatures are scaled such that the bulk temperature at the inlet is equal to 80 °C. A volumetric flow rate is imposed to the periodic boundary condition, which is either 3 l/min or 6 l/min. A heat flux of 156.64 kW/m² is applied to the bottom surface, which corresponds to a heat flow of 500 W on the full power module surface. A full solid heat sink part of 3 mm is included in the simulation domain, to allow for the uniform heat flux to spread over the different parts of the heat sink.

The fluid used for the simulation is the e-fluid Evogen5191SA and its properties at 80 °C are given in table 1. The temperature dependency of the fluid properties is also taken into account by implementing equations (1) to (4), where ρ is the density, T_f is the fluid temperature, c_p is the specific heat capacity, k is the thermal conductivity and υ is the kinematic viscosity. The solid is aluminium alloy with a thermal conductivity of 140 W/mK.

$$\rho = 1009.621\, kg\, m^{-3} - 0.6295\, kg\, m^{-3} K^{-1}\, T_f \tag{1}$$

$$c_p = 922.175\, J\, kg^{-1} K^{-1} + 3.787\, J\, kg^{-1} K^{-2}\, T_f \tag{2}$$

$$k = 0.204\, W\, m^{-1} K^{-1} - 1.822\; 10^{-4}\, W\, m^{-1} K^{-2}\, T_f \tag{3}$$

$$\nu = 1.44369\; 10^{-9}\, m^2 s^{-1}\, e^{3177.237/T_f} \tag{4}$$

Table 1. Fluid properties at 80 °C.

ρ	c_p	k	υ
787.31 kg m^{-3}	2259.6 J kg^{-1}K^{-1}	0.13966 W m^{-1}K^{-1}	11.661 10^{-6} m^2 s^{-1}

2.3. Numerical method
Ansys Fluent is employed to conduct the CFD simulations. The simulations specifically involve laminar and steady-state conditions, aligning with the desired flow regime. The maximal Reynolds number for the simulations is 87, indicating the laminar flow hypothesis is valid. The governing equations are the continuity, momentum, and energy equations. The solution process utilizes second-order discretization schemes to solve the mass, momentum, and energy conservation equations.

The simulation domain is discretized by first meshing the surface on the interface between solid and fluid with triangular elements with a size of 0.04 mm. In the fluid near the interfaces with the solid, an inflation layer is added to ensure properly capturing the boundary layers. The volumes of the solid and fluid are subsequently meshed with tetrahedral elements with a maximal size of 0.08 mm. This results in a mesh with a total of 5.4 million cells.

The grid convergence is verified by calculating Roache's grid convergence index (GCI) [5]. A simulation (with flow rate 6 l/min) is done with a coarse grid with sizing doubled compared to the fine grid and with half the amount of inflation layers. This resulted in a mesh of 0.86 million elements. The results are shown in table 2. The GCI for the fine grid is equal to 0.3% for the thermal resistance and 0.9% for the pumping power (calculated with equations (5) and (6)), which is more than sufficiently accurate for the analyses in this work.

Table 2. Grid convergence index.

	Coarse	Fine	GCI
R	0.024269 K/W	0.024341 K/W	0.3%
P	3.5153 W	3.4852 W	0.9%

3. Simulation results

3.1. Base case
The dimensions of the base case were determined based on best guesses from heat sink design experience [6]. They are given in table 3. The simulations for this case were done for two flow rates: 3 l/min and 6 l/min.

Table 3. Geometric parameters base case baffle heat sink.

A	B	C	D	E	F	G	H
0.5 mm	1 mm	1 mm	1 mm	0.5 mm	2 mm	4.5 mm	6.5 mm

Figure 3 shows the streamlines for the base case at a flow rate of 3 l/min, with the colours indicating the local velocity. It is clear that the swirling motion is induced in the bulk flow. However, for this geometry there is little flow through the top part of the heat sink. Figure 4 shows the heat flux at the solid-fluid interface from two viewpoints. On the left, the view is along the flow direction and from the left, while the figure on the right shows the view against the flow direction and from and right. The leading surfaces of the baffles exhibit high heat fluxes, as the flow impacts directly on the surfaces, while the trailing surfaces have lower heat fluxes. At the base, the heat flux is relatively high indicating the baffles aid in breaking down the thermal boundary layer. At the top of the baffles the heat flux is low, resulting from the lower velocities in this region.

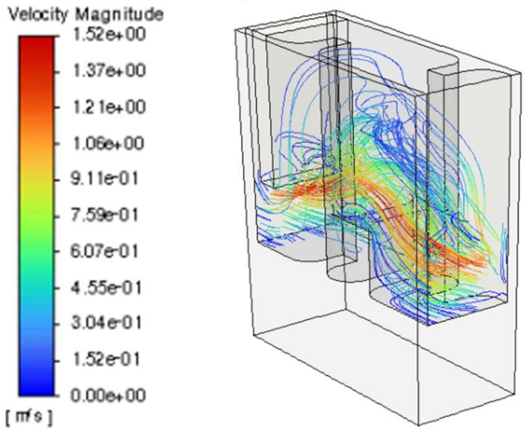

Figure 3. Streamlines with colours indicating velocity.

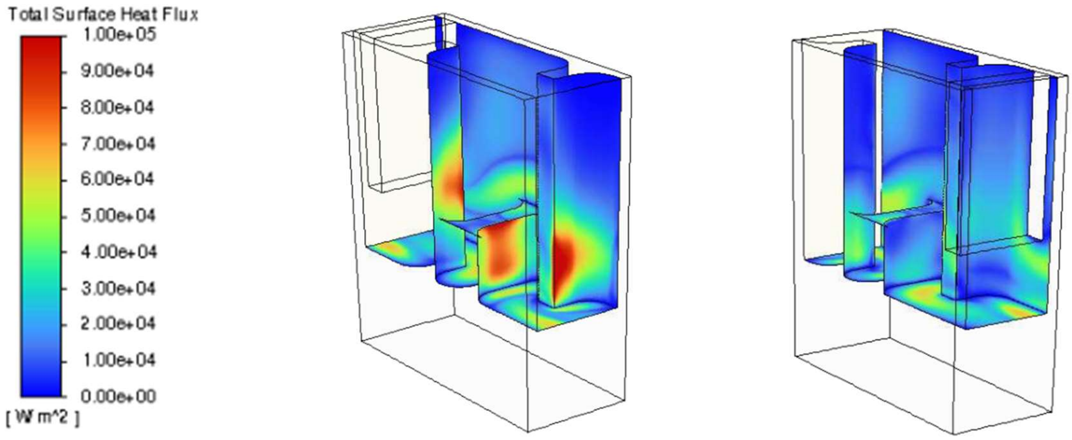

Figure 4. Heat flux at solid-liquid interface. Front-left view (left) and back-right view (right).

The heat sink is evaluated based on two criteria: thermal resistance R and required pumping power P. The thermal resistance is calculated based on equation (5), which uses the area-averaged temperature at the base in contact with the fluid T_b, the inlet temperature T_i and the total heat flow Q. A correction is made to account for the heating of the fluid along the streamwise length, using the volumetric flow rate V. The pumping power is calculated as the product of the pressure drop and volumetric flow rate as in equation (6). The pressure drop is determined from the simulations by multiplying the streamwise pressure gradient $\mathrm{d}p/\mathrm{d}x$ with the total heat sink length L.

$$R = \frac{T_b - T_i}{Q} + \frac{1}{2\,V\,\rho\,c_p} \tag{5}$$

$$P = -\frac{\mathrm{d}p}{\mathrm{d}x}\,L\,V \tag{6}$$

Figure 5 shows the thermal resistance as a function of pumping power for the base case baffle heat sink (orange square markers). An optimal heat sink has low thermal resistance and low thermal pumping power, as such points closer to the origin of the axes are better solutions. To have a comparison for the baffle heat sink, also simulation results of a pin fin heat sink with the same fluid are shown with blue diamond markers for three flow rates (6 l/min, 9 l/min and 10 l/min). The geometry of the pin fin heat sink is based on the optimization done in previous work [6]. The results show a superior performance of the baffle heat sink, with the baffle heat sink exhibiting a higher pumping power at identical flow rate.

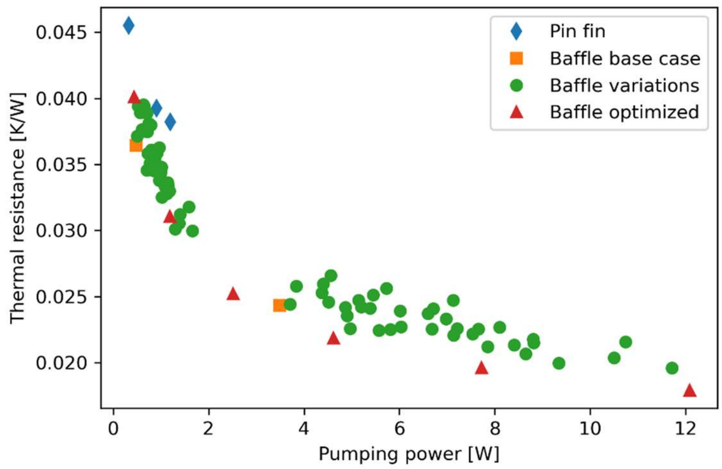

Figure 5. Thermal resistance as a function of pumping power for different heat sinks.

3.2. *Geometry optimization*

The qualitative analysis of the base case baffle heat sink showed that there should be room for improvement by changing the baffle geometry. To achieve this, for each geometric parameter a reference value and a test value was defined as shown in table 4. Simulations were done with these parameters changed one at a time and also with combinations of two parameters, resulting in 37 different geometries. Each geometry was simulated for 3 l/min and 6 l/min resulting in 74 simulations.

The thermal resistance and pumping power of these 74 cases is shown in figure 5 (green circular markers). From these simulations, it was concluded that the fin thickness, horizontal baffle spacing and baffle length should be as small as possible. The fin height, upward and downward baffle spacing, streamwise baffle spacing and baffle thickness all had optimal values. Using these conclusions, and optimal design was defined. The geometrical parameters are shown in table 4 and the geometry is shown in figure 6. Both the spacings and thicknesses were constrained to a minimal value of 0.5 mm to allow for manufacturing by milling.

Table 4. Geometric parameters of the baffle heat sinks.

Parameter	A	B	C	D	E	F	G	H
Reference	0.5 mm	1 mm	1 mm	1 mm	0.5 mm	2 mm	2 mm	6.5 mm
Test	0.3 mm	0.75 mm	0.75 mm	0.75 mm	0.3 mm	1 mm	3 mm	5 mm
Optimal	0.5 mm	0.5 mm	0.5 mm	0.9 mm	0.6 mm	1.9 mm	2.1 mm	4 mm

The optimal geometry was simulated for six different flow rates (from 2 l/min to 7 l/min in steps of 1 l/min). The streamlines with colours indicating the local velocity are shown in figure 7 for a flow rate

Journal of Physics: Conference Series **2766** (2024) 012175 doi:10.1088/1742-6596/2766/1/012175

of 2 l/min. The swirling motion is still present while it is also clear that the main fluid flow is now forced through the entire heat sink. The thermal resistance and pumping power are shown on figure 5 (red triangular markers). At equal pumping power of 1.2 W, the thermal resistance is 19% lower for the optimized baffle heat sink than for the optimized pin fin heat sink.

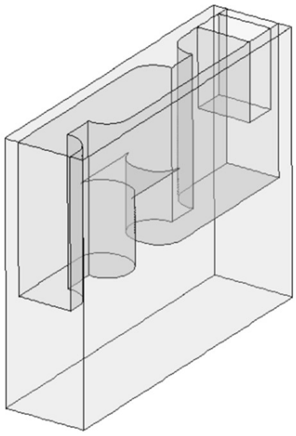

Figure 6. Unitary cell of the optimized baffle heat sink.

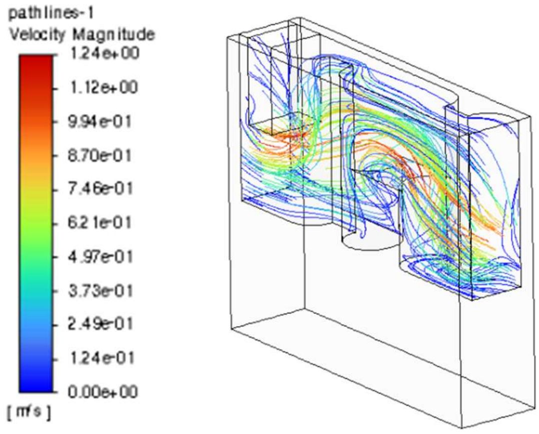

Figure 7. Streamlines with colours indicating velocity of the optimized baffle heat sink.

4. Conclusion

A novel heat sink configuration tailored for laminar flows was developed and refined, featuring baffles strategically positioned to direct flow in four distinct directions. This approach offers dual benefits: the baffles serve as fins, augmenting the heat transfer area, and induce a swirling motion in the oil flow, continuously disrupting boundary layers. Computational fluid dynamics simulations conducted with Ansys Fluent are used to assess the thermohydraulic efficacy of the baffle heat sink design.

Various combinations of design parameters are explored and it was concluded that minimizing fin thickness, horizontal baffle spacing, and baffle length is advantageous, whereas optimal values exist for fin height, upward and downward baffle spacing, streamwise baffle spacing, and baffle thickness. From these guidelines, an optimal baffle heat sink geometry was defined. Simulation results demonstrate that the thermal resistance of the optimized baffle heat sink is 19% lower compared to a benchmark pin fin heat sink under equal pumping power conditions.

Acknowledgement

This research was supported by Flanders Make, the strategic research center for the manufacturing industry, and the HERMESFONDS in the framework of the SingleOilCnL project (HBC.2020.2009).

References

[1] Pevec D, Babic J and Podobnik V 2019 Electric Vehicles: A Data Science Perspective Review, *Electronics* **8** 1-30
[2] Kempton W 2016 Electric vehicles: Driving range, *Nat. Energy* **1** 1-2
[3] Rajashekara K 2013 Present Status and Future Trends in Electric Vehicle Propulsion Technologies, *IEEE J. Emerg. Sel. Top. Power Electron.* **1** 3-10
[4] Rogiers J, T'Jollyn I, Schoonjans T, Nonneman J and De Paepe M 2022 Experimental Study on the Thermohydraulic Performance of Oil-Cooled Heat Sinks for Power Electronics *28th Int. Workshop on Thermal Investigations of ICs and Systems (THERMINIC)*
[5] Roache PJ 1997 Quantification of Uncertainty in Computational Fluid Dynamics, *Annu. Rev. Fluid Mech.* **29** 123-60
[6] Vander Heyde J, T'Jollyn I, Rogiers J, Schoonjans T, Nonneman J, Schlimpert S and De Paepe M 2021 A Comparison of the Thermohydraulic Performance of Oil-Cooled Heat Sink Geometries for Power Electronics *27th Int. Workshop on Thermal Investigations of ICs and Systems (THERMINIC)*